

UCSF

UC San Francisco Previously Published Works

Title

Expression profiling of Aldh1l1-precursors in the developing spinal cord reveals glial lineage-specific genes and direct Sox9-Nfe2l1 interactions.

Permalink

<https://escholarship.org/uc/item/3h64q2bs>

Journal

Glia, 61(9)

Authors

Glasgow, Stacey

Chaboub, Lesley

Tsai, Hui-Hsin

et al.

Publication Date

2013-09-01

DOI

10.1002/glia.22538

Peer reviewed



Published in final edited form as:

Glia. 2013 September ; 61(9): 1518–1532. doi:10.1002/glia.22538.

Expression Profiling of Aldh1l1-Precursors in the Developing Spinal Cord Reveals Glial Lineage-Specific Genes and Direct Sox9-Nfe2l1 Interactions

Anna V. Molofsky^{1,2}, Stacey M. Glasgow³, Lesley S. Chaboub⁴, Hui-Hsin Tsai^{1,5}, Alice T. Murnen¹, Kevin W. Kelley¹, Stephen P.J. Fancy¹, Tracy J. Yuen¹, Lohith Madireddy⁶, Sergio Baranzini⁶, Benjamin Deneen^{3,4,7}, David H. Rowitch^{1,5}, and Michael C. Oldham⁸

¹Department of Pediatrics, Eli and Edythe Broad Center of Regeneration Medicine and Stem Cell Research, University of California San Francisco, 513 Parnassus Avenue, San Francisco, California

²Department of Psychiatry, Langley Porter Psychiatric Institute, University of California San Francisco, 401 Parnassus Avenue, San Francisco, California

³Center for Cell and Gene Therapy, Baylor College of Medicine, One Baylor Plaza, Houston, BCM215, Texas

⁴Program in Developmental Biology, Baylor College of Medicine, One Baylor Plaza, Houston, BCM215, Texas

⁵Howard Hughes Medical Institute, University of California San Francisco, 513 Parnassus Avenue, San Francisco, California

⁶Department of Neurology, University of California San Francisco, 675 Nelson Rising Lane, Suite 215, San Francisco, California

⁷Department of Neuroscience, Baylor College of Medicine, One Baylor Plaza, Houston, BCM215, Texas

⁸Department of Neurology, Eli and Edythe Broad Center of Regeneration Medicine and Stem Cell Research, University of California San Francisco, 513 Parnassus Avenue, San Francisco, California

Abstract

Developmental regulation of gliogenesis in the mammalian CNS is incompletely understood, in part due to a limited repertoire of lineage-specific genes. We used Aldh1l1-GFP as a marker for gliogenic radial glia and later-stage precursors of developing astrocytes and performed gene expression profiling of these cells. We then used this dataset to identify candidate transcription factors that may serve as glial markers or regulators of glial fate. Our analysis generated a database of developmental stage-related markers of Aldh1l1+ cells between murine embryonic day 13.5–18.5. Using these data we identify the bZIP transcription factor *Nfe2l1* and demonstrate that it promotes glial fate under direct Sox9 regulatory control. Thus, this dataset represents a resource for identifying novel regulators of glial development.

© 2013 Wiley Periodicals, Inc.

Address correspondence to David H. Rowitch, University of California San Francisco, 513 Parnassus Avenue, San Francisco, CA 94143. RowitchD@peds.ucsf.edu and Michael C. Oldham, University of California San Francisco, 513 Parnassus Avenue, San Francisco, CA 94143. OldhamM@stemcell.ucsf.edu.

Anna V. Molofsky and Stacey M. Glasgow contributed equally.

Additional Supporting Information may be found in the online version of this article.

Keywords

astrocytes; gliogenesis; expression profiling; gene coexpression; Nfe2l1

Introduction

Astrocytes and oligodendrocytes play major roles in adult brain function, yet much remains to be learned about their specification and early development. It is increasingly clear that astrocytes and their precursors play critical roles in normal neurodevelopment including promoting synaptogenesis (Christopherson et al. 2005; Pfrieger 2009; Ullian et al. 2001), axon integrity (Edgar and Nave, 2009), response to injury (Sofroniew and Vinters, 2010) and myelination (Meyer-Franke, 1999; Watkins et al., 2008).

Astrocytes have been implicated in neurodevelopmental diseases including Rett Syndrome (Ballas et al., 2009; Liroy et al., 2011), Fragile X syndrome (Jacobs and Doering, 2010), Schizophrenia (Pantazopoulos et al., 2010), and others (Molofsky et al., 2012). Astrocytes are first generated from radial glial progenitors following the cessation of neurogenesis (Rowitch and Kriegstein, 2010). These progenitors delaminate and move into the parenchyma, where they become astrocyte precursors that morphologically resemble parenchymal astrocytes. In spinal cord, astrocytes are produced from all dorsal–ventral regions (Tsai et al., 2012), whereas oligodendrocytes are initially produced from the ventral “pMN” domain (Lu et al., 2002; Zhou and Anderson, 2002) and in dorsal domains at later stages (Cai et al., 2005; Fogarty et al., 2005; Vallstedt et al., 2005).

A major limitation in understanding glial development is the lack of markers to prospectively isolate glial progenitors at embryonic stages. Studies of the astrocyte lineage have classically relied on expression of glial fibrillary acidic protein (Gfap), a marker of terminally differentiated astrocytes (Bignami et al., 1972). However, Gfap is not expressed at the stage of astrocyte specification, and therefore does not function as a pan-lineage or lineage-specific marker. Other reported factors, while important in astrocyte development, are not specific to the astrocyte lineage and thus fail as prospective markers. These include Nfia (Deneen et al., 2006), Sox9 (Stolt et al., 2003), and Fgfr3 (Pringle and Richardson, 1993).

Aldh1l1 is a folate metabolic enzyme identified by transcriptional profiling as a bona fide astrocyte marker (Cahoy et al., 2008) that does not colabel with markers of other mature cell types in postnatal brain and is broadly expressed in both fibrous and protoplasmic astrocytes (Yang et al., 2010). Aldh1l1-GFP is first detected in the spinal cord in radial glial precursors around the time of the neuron-glia switch at mE12.5, and generalizes thereafter to label parenchymal cells (Anthony and Heintz, 2007) which are astrocyte precursors (Tien et al., 2012; Tsai et al., 2012). We sought to use Aldh1l1 as a marker of early gliogenic populations in order to identify genes associated with glial development. To this end, we used the Aldh1l1-GFP BAC transgenic mouse (Heintz, 2004) to perform microarray analysis of highly purified flow-sorted populations of Aldh1l1-positive spinal cord cells from E13.5–18.5, the period spanning early and active gliogenesis (Tien et al., 2012).

We performed gene coexpression analysis (Oldham et al., 2008; Zhang and Horvath, 2005) of this dataset and identified three temporally distinct patterns of gene activity, or “modules,” in Aldh1l1-positive spinal cord cells. These modules were temporally correlated with early, middle, and late embryogenesis, and were strongly enriched for genes known to be associated with astrocyte development. Pathway analysis revealed that early glial genes are strongly enriched for axon guidance molecules, whereas in late embryogenesis genes that influence neuronal signaling predominate. By searching for transcription factors

associated with each temporal profile, we identified *Nfe2l1* as a novel gliogenic transcription factor, which we show promotes astrocyte and oligodendrocyte maturation as part of a Sox9 regulatory program. This example illustrates the utility of this dataset as a ready resource for further discovery of genes involved in gliogenesis.

Materials and Methods

Mice

Aldh1l1-GFP transgenic mice generated by the GENSAT project were backcrossed for >5 generations onto a Swiss-Webster background and housed in accordance with UCSF policies. Plug date was considered embryonic day 0.5, and age was confirmed by morphology and crown-rump length measurements at harvest. Microarray samples were collected from 3 E13.5 embryos, 2–3 E14.5 embryos, and 3 E17.5–18.5 embryos. Neurospheres from Fig. 6c were generated from E13.5 Sox9^{fllox/fllox};Nestin-cre (KO) and Sox9^{fllox/+};Nestin-cre (HET).

Flow Cytometry

Spinal cords were dissected and dorsal root ganglia and meninges removed, then dissociated with papain 20 U/mL (Worthington) for 80 minutes at 33°C as previously described (Cahoy et al., 2008). Aldh1l1-positive and -negative cells were sorted on a BD FACS Aria II and gated on forward/side scatter, live/dead by DAPI exclusion, and GFP, using GFP-negative and DAPI-negative controls to set gates for each experiment. GFP-positive populations were re-sorted using the same gates.

RNA Isolation and Microarray Analysis

RNA from 35,000–200,000 cells per sample was isolated using TRI-ZOL reagent (Invitrogen), DNase digested to remove genomic DNA contamination, and further purified using the RNAeasy Kit (Qiagen). For microarray analysis, RNA samples were amplified using the Nugen Pico WT Ovation Kit and hybridized to Affymetrix Mouse Gene 1.0 ST arrays.

Bioinformatics

Microarray data were preprocessed in R using the Bioconductor suite of software packages. The “oligo” package was used to background correct, normalize, and summarize probes at the transcript level via the Robust Multi-array Analysis (RMA) algorithm (Irizarry et al., 2003). Control probe sets and probe sets without annotations were removed. For probe sets with duplicate annotations, the one with the highest variance across all samples was retained. Quality control was performed on the resultant 23,890 probe sets using the SampleNetwork R function (Oldham et al., 2012). This analysis revealed one outlier sample (E14.5 Aldh1l1+), which was removed from the analysis. Expression data were reverse log-transformed, then gene coexpression modules were identified using a four-step approach. First, pairwise Pearson correlation coefficients (cor) were calculated across all 17 samples. Second, transcripts were clustered using the flashClust (Langfelder and Horvath, 2008) implementation of a hierarchical clustering procedure with complete linkage and 1–cor as a distance measure. The resulting dendrogram was cut at a static height of ~0.327 (corresponding to the top 2% of pairwise correlations). Third, clusters of at least 20 members were summarized by their module eigengene (i.e., the first principal component obtained via singular value decomposition (Horvath and Dong, 2008; Oldham et al., 2006)). Fourth, highly similar modules were merged if their Pearson correlation coefficients exceeded an arbitrary threshold (0.8). This procedure was performed iteratively until no pairs of modules exceeded the threshold. This yielded 10 coexpression modules, for which

the strength of module membership (k_{ME}) for each transcript was calculated by correlating its expression pattern across all samples with each module eigengene (Horvath and Dong, 2008; Oldham et al., 2008). The MAPPER search engine (Marinescu et al., 2005) was used for promoter analysis as previously described (Kang et al., 2011).

Immunohistochemistry/In Situ Hybridization

Antibodies used included mouse anti-NeuN (Millipore 1:100) mouse anti-Olig2 1:100 and rabbit anti-Olig2 1:10,000 (gifts of C. Stiles), rabbit monoclonal anti-Id3 1:1000 (Biocheck clone 4/17-3), and chick anti-GFP 1:500 (Aveslabs). Heat-mediated antigen retrieval for Id3 was optimized to preserve GFP antigenicity by 10 minutes at 70° in citrate buffer. *In situ* hybridization probes used were cFABP7, cGLAST, cPDGFR α , mNfe211, and mAldh111. Mouse probes were generated using primer and sequence information from the Allen Brain Atlas (Lein et al., 2007).

Cell Culture

E14.5 mouse telencephalon was dissociated and plated at high density in neural stem cell medium containing 20 ng/mL FGF, 20 ng/mL EGF, and 10% chick embryo extract, as previously described (Molofsky et al., 2003). After 24 hours cultures were infected with a pMIG retrovirus (mouse stem cell virus, Addgene.org) containing the transcription factor coding sequence (human Nfe211, others) and an IRES-GFP. Cells were repassaged into clonal density cultures 24–48 hours after infection. Neurosphere cultures were generated by plating into ultra-low adhesion plates (Corning,) and adherent cultures were generated by plating 800 cells per well of a six well plate coated with poly-D-lysine and fibronectin (Biomedical technologies, Stoughton, MA). Neurospheres were self-renewed by mechanical dissociation and passaging after 10 days in culture. Adherent colonies were cultured for the time periods indicated then fixed in 4% paraformaldehyde and stained for O4 (ATCC), Tuj1 (Covance), and GFAP (DAKO).

Chick Electroporation

Chick electroporation was performed as previously described (Kang et al., 2011). Briefly, expression constructs were cloned into the RCAS(B) using gateway cloning (Invitrogen) (Morgan and Fekete, 1996). Constructs were injected into the chick spinal cord at stage HH13–HH15 (~cE2). Electroporation was carried out with a BTX Electro Square Porator (Momose et al., 1999). Three days (cE5) or five days (cE7) post-electroporation, spinal cords were harvested, fixed in 4% PFA and sunk in 20% sucrose.

qPCR and ChiP

Harvested P19 cells were fixed with 1% formaldehyde for 10 minutes. Cross-linked chromatin was then sheared by sonication and cleared by centrifugation. The samples were precleared with protein G beads and immunoprecipitated using Sox9 antibody (Millipore) or control IgG (Santa Cruz Biotechnology). Immunoprecipitated complexes were isolated, the cross-links reversed, and proteins digested with proteinase K. The DNA was purified and PCR was performed using region-specific primers. ChIP primers for Nfe211: Upstream: Fwd-AATCAGATAGCCGGACTAGAG, Rev-CAATGCTCCAT-TATCTGCCTTA; Intron element: Fwd-GCCTGTTACCTAGCTG-CAGAA; Rev-GAGGACTAGCCATCGTCTTCTT.

Total RNA was isolated from mouse neurospheres using a RNeasy mini isolation kit (Qiagen). Superscript III (Invitrogen) was used for reverse transcription of 1 μ g of total RNA samples. Quantitative RT-PCR was performed using PerfeCta SYBR Green Fast Mix (Quanta Biosciences) and a LightCycler 480 (Roche).

qPCR primers: cyclophilin: Fwd-GTCTCCTTCGAGCTGT TTGC; Rev-GATGCCAGGACCTGTATGCT; Nfe2L1: Fwd-TCG GTGAAGATTTGGAGGA; Rev-GTCGCCAAAGGATGTCAATC.

Results

Developmental Expression of Aldh111-eGFP as a Glial Lineage Marker

To validate Aldh111-eGFP as a marker for flow-cytometric isolation of glial precursors, we examined embryonic sections from Aldh111-GFP BAC transgenics from the GENSAT project (Gong et al., 2003). In the spinal cord, Aldh111-GFP was first detected in ventricular zone radial glia at ~E13.5, where it partly colabeled with the oligodendrocyte precursor marker Olig2. By E18.5 expression was exclusively detected in a parenchymal population with astrocytic morphology (Fig. 1a–c, see also (Tsai et al., 2012; Tien et al., 2012).) In the forebrain, onset of Aldh111 expression was delayed relative to the spinal cord, and both “radial glial-like” and “astrocyte-like” Aldh111-GFP positive cells coexisted into postnatal stages (not shown). Due to this heterogeneity in the fore-brain, we focused our ensuing analysis on spinal cord.

To characterize this developmental window of gliogenesis, spinal cords were enzymatically dissociated and Aldh111-GFP positive cells were isolated from spinal cord at E13.5 ($n = 3$), E14.5 ($n = 3$), and E17.5–18.5 ($n = 3$; Fig. 1d–f), during which the percentage of Aldh111-GFP positive cells increased from 8 to 36%. GFP-positive samples were resorted for increased purity (>90% after the first sort and >95% after the second; Fig. 1g). Control samples consisted of whole spinal cord sorted using only scatter and viability gates from each of these timepoints. RNA from a total of 18 samples (9 Aldh111-positive and 9 whole spinal cord controls) was hybridized to Affymetrix Mouse Gene 1.0 ST arrays, and 17 were retained for further analysis.

Fate mapping using Aldh111-cre has previously demonstrated that >80% of Aldh111-positive cells in the spinal cord become glia, while a small percentage become interneurons (Tien et al., 2012); thus Aldh111-eGFP is highly selective, but not exclusive, to glial populations during embryogenesis. Consistent with these findings, our microarray data revealed high expression levels in Aldh111-positive cells of early astrocyte markers, including Aldoc, Slc1a3 (glast), and Gja1 (connexin 43), which also increased with time (Fig. 1h). Markers typically associated with mature astrocytes, including Aqp4 and Gfap, were detected at low levels at E17.5–18.5 but not earlier (Fig. 1h). Neuronal markers such as Syt1, Snap25, and Nefl were detected at very low levels throughout (Fig. 1i).

Gene Coexpression Analysis of Developing Spinal Cord Yields Modules that Segregate into Astrocytic and Neuronal Subtypes

To identify groups of genes with similar temporal patterns of activity during glial development, we performed gene coexpression analysis (Oldham et al., 2008; Zhang and Horvath, 2005). Unlike differential expression analysis, which is a univariate technique that seeks to compare mean expression levels for individual genes between groups of samples, coexpression analysis is a multivariate technique that organizes genes into “modules” that share significant covariation. Coexpression analysis has been shown to be a powerful tool for deconvolving molecular signatures of distinct CNS cell types in heterogeneous tissue samples (Oldham et al., 2006, 2008).

We analyzed gene coexpression relationships in flow-sorted Aldh111-GFP positive cells and whole spinal cord at E13.5, E14.5, and E17.5–18.5. This analysis identified 10 modules of genes with coordinated expression activity across samples. We summarized the

characteristic pattern of gene activity for each module by calculating its first principal component, or “module eigengene” (Horvath and Dong, 2008; Oldham et al., 2006). Hierarchical clustering of the module eigengenes revealed a bifurcation between modules with higher expression levels in Aldh111-positive samples compared with whole spinal cord, or vice versa (Supp. Info. Fig. 1).

Gene Coexpression Analysis Reveals Three Temporal Waves of Glial Genes

We focused our subsequent analysis on four of five modules that showed high expression levels in Aldh111-positive samples relative to whole spinal cord. A complete description of the correlations between each of these modules and all genes on the microarray is available as Supporting Information Table 1. Plots of the module eigengenes revealed how these genes were correlated across developmental time (Fig. 2). Three of these modules were highly enriched for genes associated with astrocyte development and maturity that temporally segregated into early, middle, and late embryogenesis.

Genes in first module (Fig. 2a), the “early” module, were highly expressed in Aldh111-positive samples at E13.5-E14.5 and decreased sharply thereafter, with low expression in whole-cord samples. This module includes proposed early astrocyte markers such as Slit1 (Hochstim et al., 2008), and radial glial markers such as vimentin (Roeling and Feirabend, 1988) and Ctnnb1 (beta-catenin). Thus, this module may include other genes involved in the transition from radial glia to glial progenitor.

The second and largest of the modules is the “middle” module (Fig. 2b). Genes in this module were highly expressed in Aldh111-positive cells throughout embryogenesis. Many are genes involved in early glial specification, including Slc1a3 (glast) (Shibata et al., 1997; Regan et al., 2007), Fgfr3 (Pringle et al., 2003), AldoC (Walther et al., 1998), Aldh111 (Cahoy et al., 2008), Sox9 (Stolt et al., 2003), and Nfia (Deneen et al., 2006).

The third temporal module is the “late” module (Fig. 2c). These genes were expressed only during late embryogenesis, increasing approximately fourfold from the earliest time point. As expected, genes in this module include many canonical markers of terminal astrocyte differentiation, such as Apoe (Xu et al., 2006), Cldn10, Aqp4 (Nielsen et al., 1997), Slc1a2 (glt-1) (Furuta et al., 1997), Acsbg1 (bubble-gum) (Song et al., 2007), Gja1 (a.k.a connexin43) (Giaume et al., 1991), Glud1 (Lovatt et al., 2007), Folh1 (Sácha et al., 2007), and Cd44 (Liu et al., 2004).

Interestingly, one additional module (Fig. 2d) showed a bimodal expression peak at E13.5 and E17.5 in Aldh111-positive samples, and was highly enriched with genes involved in mitosis, including cyclins, histone genes, and microtubule-associated proteins. This module suggests that Aldh111-positive cells undergo two periods of active cell division with a period of relative quiescence at E14.5. We have validated this hypothesis *in vivo* by quantifying colabeling with phosphohistone H3 (Tien et al., 2012).

As a means of gene discovery, our gene coexpression analysis demonstrates in a prospective way that there are distinct groups of genes associated with early, middle, and late embryonic glial development. Analysis of well known genes in each group allowed us to determine the “character” of the module and select novel genes for further analysis. As will be shown below, the grouping of astrocyte genes into early, middle, and late modules allows us to make both general and specific observations about genes involved in glial development.

Pathway Analysis Suggests Functional Differences Between Early, Middle, and Late Gliogenic Genes

We performed Ingenuity Pathways Analysis (Ingenuity® Systems, www.ingenuity.com) to screen for functional classes of genes that might be unique to glia at different stages of maturation. This analysis suggested different functional roles for glia at different developmental stages (Table 1). For example, we found that axon guidance pathways, including ephrin/eph receptor signaling, were strongly represented in the early module. The middle module had many pathways associated with active biosynthesis including fatty acid beta oxidation, valine degradation, and oleate biosynthesis. The late module likely represents an early population of maturing astrocytes that persists into the postnatal period. This module was significantly enriched with pathways including GABA receptor signaling, choline biosynthesis, and long-term depression, consistent with possible roles of early post-natal astrocytes in modulation of neuronal signaling and synaptic plasticity.

Gene Ontology Analysis of Coexpression Modules Reveals Transcription Factor Nuclear Markers of Developing Astrocytes

We used Ingenuity Pathways Analysis to annotate putative transcription factors that were highly correlated with each temporal module (Table 2). The top transcription factor in the middle module was Id3, which has been detected in other astrocyte screens (Cahoy et al., 2008; Fu et al., 2009) and has been proposed as an astrocyte-specific marker (Muroyama et al., 2005; Tzeng and de Vellis, 1997, 1998). We validated Id3 as a marker of developing astrocytes using two novel reagents that may prove useful to studying astrocyte function (Fig. 3). First, we tested a GENSAT Id3-GFP mouse (Heintz, 2004) against markers of astrocytes, oligodendrocytes, and neurons (Fig. 3a–d) and found that it is specific for the astroglial lineage. We then tested several Id3 antibodies for specificity against the Id3-GFP mouse and found one that was useful for nuclear labeling of developing astrocytes (Fig. 3e–i). Interestingly, Id3 protein was downregulated with astrocyte maturation (Fig. 3j), suggesting that it is a marker of developing, but not mature astrocytes. Consistent with previous transcript analyses (Tzeng et al., 2001), we found robust Id3 nuclear protein expression in the context of demyelinating injury-induced reactive gliosis (Fig. 3k, k'). Thus, Id3-GFP mouse could be a useful tool for identification and flow-cytometric isolation of reactive astrocytes *in vivo*.

The Transcription Factor Nfe2l1 Promotes Glial Maturation

To further validate this dataset as a useful means of identifying transcription factors relevant to glial development we next devised a functional screen to identify transcription factors in the early and middle modules that could promote glial specification or maturation. Coding sequences for selected transcription factors from Table 2 were cloned into a retrovirus with an IRES-GFP (MSCV) and overexpressed in clonal neural stem cell colonies (Fig. 4b). *In vitro* culture of telencephalic progenitors in the presence of growth factors is a well-characterized system for studying neural stem cells (Molofsky et al., 2003). In adherent clonal cultures over 80% of colonies derived from individual tel-encephalic progenitors are multipotent and express markers of neurons, astrocytes, and oligodendrocytes, and the neurosphere generated under nonadherent conditions can be passaged *in vitro* as a measure of the self-renewal potential of the founder stem cell. Overexpression of putative glial-specification genes in this system provides a quantifiable way to test whether these genes promote differentiation of neural stem cells.

We reasoned that gliogenic transcription factors would accelerate differentiation in neural stem cell colonies, thereby leading to decreased self-renewal and precocious expression of glial, but not neuronal, markers. Using this approach, we screened several candidate transcription factors by misexpression in multipotent neural stem cell colonies. Some factors

were strongly selected against in this system due to proapoptotic or antiproliferative effects (not shown). One factor from the middle module, HopX, did not decrease self-renewal, but modestly increased the expression of astrocyte and oligodendrocyte, but not neuronal markers (Supp. Info. Fig. 2). Interestingly, an independent screen of gliogenic transcription factors also identified HopX (a.k.a. Hod-1) and demonstrated that it is downregulated in Sox9 and Nfia deficient neurospheres (Kang et al., 2011).

We subsequently focused on the top transcription factor in the early module, the bZIP transcription factor *Nfe2l1* (Murphy and Kolst^r, 2000). We confirmed that *Nfe2l1* is expressed in the ventricular zone at E13.5 (Fig. 4a) and decreases thereafter with a subsequently neuronal expression pattern (not shown). Overexpression of *Nfe2l1* in neural stem cell colonies led to a twofold decrease in neurosphere self-renewal (Fig. 4c). To test whether this was associated with accelerated fate commitment, we quantified lineage marker expression at 7, 9, and 12 days in culture ($n = 4$ independent experiments). Overexpression of *Nfe2l1* did not increase the rate of neuronal marker expression (Tuj1+, Fig. 4d), suggesting that it does not generically promote differentiation; however, it significantly accelerated the rate at which colonies acquired astrocyte (Gfap) and oligodendrocyte (O4) marker expression (Fig. 4e–h). By 13 days these differences were no longer significant, suggesting that *Nfe2l1* is not simply promoting the survival of glial-restricted progenitors.

To test whether *Nfe2l1* could promote glial fate *in vivo*, we generated an Nfe2l1-RCAS construct for overexpression in chick neural tube. Neural tubes were electroporated at chick embryonic day 2 with either Nfe2l1 or empty vector and spinal cords were harvested at cE5 and cE7 (Fig. 5), before and after the gliogenic switch, respectively. Electroporation of Nfe2l1-RCAS did not increase the expression of astrocytic specification markers Fabp7 and Glast (Fig. 5b, c, g, h), and precocious Gfap expression was not detected (data not shown). However, Nfe2l1 did induce expression of the early oligodendrocyte marker PDGFR α at cE5 (Fig. 5d) in 6/6 embryos tested, and the mature oligodendrocyte marker MBP at cE7 (Fig. 5j) compared with empty vector controls. No difference was detected in Olig2 staining (Fig. 5e), suggesting that Nfe2l1 may be affecting oligodendrocyte maturation rather than specification, although loss-of-function studies would be needed to further assess this possibility. In summary, *Nfe2l1* was expressed in the ventral neural tube during early gliogenesis and stimulated expression of astrocyte and oligodendrocyte markers *in vitro*, and oligodendrocyte markers *in vivo*, suggesting a role in promoting glial fate.

Nfe2l1 is Positively Regulated by Sox9

Given the role of *Nfe2l1* in promoting gliogenesis and its temporal expression pattern, we hypothesized that Nfe2l1 expression may be regulated by Sox9, which plays a critical role in the initiation of gliogenesis (Stolt et al., 2003). To explore this question, we analyzed *Nfe2l1* promoter sequence and identified several putative Sox9-binding sites (Fig. 6a). Using an antibody to Sox9 we performed Chromatin Immunoprecipitation (ChIP) from the P19 multipotent cell line, which mimics endogenous differentiation and can be driven to an oligodendrocyte or astrocyte cell-fate (McBurney, 1993). We found that Sox9 associates with the predicted Sox binding sites in the *Nfe2l1* promoter (Fig. 6b). To test whether this association might have functional relevance, we quantified levels of Nfe2l1 in Sox9-deficient neurospheres. Strikingly, we observed a >10-fold decrease in Nfe2l1 expression in these cells relative to Sox9-heterozygous neurospheres. These data demonstrate that Sox9 directly induces Nfe2l1 expression, at least in culture. This observation is consistent with a model in which Sox9 acts to induce glial differentiation as part of a regulatory cascade that promotes the expression of glial-specific genes.

Discussion

In this study, we demonstrate that Aldh1l1 is a useful marker of gliogenic lineages during embryonic spinal cord development. Transcriptional profiling of Aldh1l1-positive populations to search for genes that are temporally correlated with the radial glial-immature-astrocyte transition revealed three temporal modules of genes: an early embryonic module, a late embryonic module, and a middle module that was pan-embryonic and strongly enriched for genes associated with glial fate determination. In order to validate gene coexpression analysis as a useful way to generate new hypotheses from a complex dataset, we chose to focus on transcription factors that were strongly associated with two of the identified temporal modules. One of these transcription factors, Id3, has been previously identified in screens of astrocyte specific genes, and was validated here using two novel astrocyte-specific reagents.

To identify genes with functional significance for gliogenesis, we focused on transcription factors in the early and middle modules, which included genes that were highly expressed in Aldh1l1-positive radial glia during early embryogenesis. Functional screening of several transcription factors in clonal neural stem cell colonies identified the transcription factor *Nfe2l1*. *Nfe2l1* (a.k.a. Nrf1, Tcf11) is a bZIP transcription factor expressed in multiple tissues throughout early embryonic development (Murphy and Kolst', 2000). Knockout mice have early embryonic lethality because of hematopoietic defects (Chan et al., 1998). Recent conditional deletion of *Nfe2l1* in the CNS via nestin-cre revealed a post-natal neurodegenerative phenotype and death by weaning. While these data may be consistent with the expression of *Nfe2l1* in neurons postnatally, possible glial defects were not specifically examined (Kobayashi et al., 2011).

We found that *Nfe2l1* is expressed in the ventricular zone during early gliogenesis and promotes acquisition of astrocyte and oligodendrocyte fate *in vitro*, and some markers of oligodendrocyte fate *in vivo*. In addition, we revealed a direct regulatory relationship between Sox9 and *Nfe2l1* in which the glial fate-specifying gene Sox9 physically associates with *Nfe2l1* (in a multipotent cell line) and promotes its expression (in cultured neurospheres). This finding suggests that *Nfe2l1* may be one of the genes that are controlled by Sox9 as part of a regulatory cascade involved in the acquisition of glial fate, although it was not possible to directly demonstrate that this interaction is occurring in multipotent progenitors *in vivo*. Further detailed loss-of-function studies will be required to further assess whether this gene is required for glial fate determination.

Interestingly, although fate mapping and gene expression analyses suggest that Aldh1l1 expression primarily marks the astrocyte lineage, our *in vitro* and *in vivo* data suggest that *Nfe2l1* modestly promotes GFAP expression *in vitro*, but promotes oligodendrocyte fate *in vitro* and *in vivo*. These results may reflect limitations of our currently available astrocyte markers to identify intermediate stages of astrocyte fate acquisition. It is also possible that factors that promote oligodendroglialogenesis when overexpressed may have more subtle roles in astrocyte specification when studied by loss-of-function analyses.

In this study, we have generated a rich dataset with which to mine the early stages of astrocytogenesis for marker discovery as well as functional analyses. The distinct temporal patterns of gene activity that we have identified in glial precursors suggest that glia undergoing the radial glia-to-progenitor transition serve defined roles in the developing nervous system, and that these roles change over time. A greater appreciation for these roles will be critical if we are to understand how glia develop, support neuronal function, and contribute to neurodevelopmental diseases.

Supplementary Material

Refer to Web version on PubMed Central for supplementary material.

Acknowledgments

Grant sponsor: National Institutes of Mental Health; Grant number: R25MH060482; Grant sponsor: the Cancer Prevention and Research Institute of Texas; Grant number: RP101499; Grant sponsor: National Institutes of Health; Grant number: R01 NS071153; 5-T32HL092332-08; Grant sponsor: University of California, San Francisco Program for Breakthrough Biomedical Research, Sandler Foundation.

Dr. E. Huillard for helpful suggestions, Sarah Luo for assistance with flow cytometry, the UCSF Genomics core facility, and the UCSF Flow cytometry core facility. S.E.B. is a Harry Weaver neuroscience scholar from the National multiple sclerosis society. The authors declare no conflicts of interest.

References

- Anthony TE, Heintz N. The folate metabolic enzyme ALDH1L1 is restricted to the midline of the early CNS, suggesting a role in human neural tube defects. *J Comp Neurol.* 2007; 500:368–383. [PubMed: 17111379]
- Bachoo RM, Kim RS, Ligon KL, Maher EA, Brennan C, Billings N, Chan S, Li C, Rowitch DH, Wong WH, DePinho RA. Molecular diversity of astrocytes with implications for neurological disorders. *Proc Natl Acad Sci USA.* 2004; 101:8384–8389. [PubMed: 1515908]
- Ballas N, Lioy DT, Grunseich C, Mandel G. Non-cell autonomous influence of MeCP2-deficient glia on neuronal dendritic morphology. *Nat Neurosci.* 2009; 12:311–317. [PubMed: 19234456]
- Bignami A, Eng LF, Dahl D, Uyeda CT. Localization of the glial fibrillary acidic protein in astrocytes by immunofluorescence. *Brain Res.* 1972; 43:429–435. [PubMed: 4559710]
- Cahoy JD, Emery B, Kaushal A, Foo LC, Zamanian JL, Christopherson KS, Xing Y, Lubischer JL, Krieg PA, Krupenko SA, Thompson WJ, Barres BA. A transcriptome database for astrocytes, neurons, and oligodendrocytes: a new resource for understanding brain development and function. *J Neurosci.* 2008; 28:264–278. [PubMed: 18171944]
- Cai J, Qi Y, Hu X, Tan M, Liu Z, Zhang J, Li Q, Sander M, Qiu M. Generation of oligodendrocyte precursor cells from mouse dorsal spinal cord independent of Nkx6 regulation and Shh signaling. *Neuron.* 2005; 45:41–53. [PubMed: 15629701]
- Chan JY, Kwong M, Lu R, Chang J, Wang B, Yen TS, Kan YW. Targeted disruption of the ubiquitous CNC-bZIP transcription factor, Nrf-1, results in anemia and embryonic lethality in mice. *EMBO J.* 1998; 17:1779–1787. [PubMed: 9501099]
- Christopherson KS, Ullian EM, Stokes CCA, Mullen CE, Hell JW, Agah A, Lawler J, Moshier DF, Bornstein P, Barres BA. Thrombospondins are astrocyte-secreted proteins that promote CNS synaptogenesis. *Cell.* 2005; 120:421–433. [PubMed: 15707899]
- Deneen B, Ho R, Lukaszewicz A, Hochstim CJ, Gronostajski RM, Anderson DJ. The transcription factor NFIA controls the onset of gliogenesis in the developing spinal cord. *Neuron.* 2006; 52:953–968. [PubMed: 17178400]
- Edgar JM, Nave K-A. The role of CNS glia in preserving axon function. *Curr Opin Neurobiol.* 2009; 19:498–504. [PubMed: 19765974]
- Fogarty M, Richardson WD, Kessaris N. A subset of oligodendrocytes generated from radial glia in the dorsal spinal cord. *Development.* 2005; 132:1951–1959. [PubMed: 15790969]
- Fu H, Cai J, Clevers H, Fast E, Gray S, Greenberg R, Jain MK, Ma Q, Qiu M, Rowitch DH, Taylor CM, Stiles CD. A genome-wide screen for spatially restricted expression patterns identifies transcription factors that regulate glial development. *J Neurosci.* 2009; 29:11399–11408. [PubMed: 19741146]
- Furuta A, Rothstein JD, Martin LJ. Glutamate transporter protein subtypes are expressed differentially during rat CNS development. *J Neurosci.* 1997; 17:8363–8375. [PubMed: 9334410]
- Giaume C, Fromaget C, Aoumari el A, Cordier J, Glowinski J, Gros D. Gap junctions in cultured astrocytes: Single-channel currents and characterization of channel-forming protein. *Neuron.* 1991; 6:133–143. [PubMed: 1702648]

- Gong S, Zheng C, Doughty ML, Losos K, Didkovsky N, Schambra UB, Nowak NJ, Joyner A, Leblanc G, Hatten ME, Heintz N. A gene expression atlas of the central nervous system based on bacterial artificial chromosomes. *Nature*. 2003; 425:917–925. [PubMed: 14586460]
- Heintz N. Gene expression nervous system atlas (GENSAT). *Nat Neuro-sci*. 2004; 7:483.
- Hochstim C, Deneen B, Lukaszewicz A, Zhou Q, Anderson DJ. Identification of positionally distinct astrocyte subtypes whose identities are specified by a homeodomain code. *Cell*. 2008; 133:510–522. [PubMed: 18455991]
- Horvath S, Dong J. Geometric interpretation of gene coexpression network analysis. *PLoS Comput Biol*. 2008; 4:e1000117. [PubMed: 18704157]
- Irizarry RA, Hobbs B, Collin F, Beazer-Barclay YD, Antonellis KJ, Scherf U, Speed TP. Exploration, normalization, and summaries of high density oligonucleotide array probe level data. *Biostatistics*. 2003; 4:249–264. [PubMed: 12925520]
- Jacobs S, Doering LC. Astrocytes prevent abnormal neuronal development in the fragile x mouse. *J Neurosci*. 2010; 30:4508–4514. [PubMed: 20335488]
- Kang P, Lee HK, Glasgow SM, Finley M, Donti T, Gaber ZB, Graham BH, Foster AE, Novitsch BG, Gronostajski RM, Deneen B. Sox9 and NFIA coordinate a transcriptional regulatory cascade during the initiation of gliogenesis. *Neuron*. 2011; 74:79–94. [PubMed: 22500632]
- Kobayashi A, Tsukide T, Miyasaka T, Morita T, Mizoroki T, Saito Y, Ihara Y, Takashima A, Noguchi N, Fukamizu A, Hirotsu Y, Ohtsuji M, Katsuoka F, Yamamoto M. Central nervous system-specific deletion of transcription factor Nrf1 causes progressive motor neuronal dysfunction. *Genes to Cells*. 2011; 16:692–703. [PubMed: 21554501]
- Langfelder P, Horvath S. WGCNA: An R package for weighted correlation network analysis. *BMC Bioinformatics*. 2008; 9:559. [PubMed: 19114008]
- Lein ES, Hawrylycz MJ, Ao N, Ayres M, Bensinger A, Bernard A, Boe AF, Boguski MS, Brockway KS, Byrnes EJ, Chen L, Chen T-M, Chin MC, Chong J, Crook BE, Czaplinska A, Dang CN, Datta S, Dee NR, Desaki AL, Desta T, Diep E, Delbeare TA, Donelan MJ, Dong H-W, Dougherty JG, Duncan BJ, Ebbert AJ, Eichele G, Estlin LK, Faber C, Facer BA, Fields R, Fischer SR, Fliss TP, Frensley C, Gates SN, Glattfelder KJ, Halverson KR, Hart MR, Hohmann JG, Howell MP, Jeung DP, Johnson RA, Karr PT, Kawal R, Kidney JM, Knapik RH, Kuan CL, Lake JH, Laramee AR, Larsen KD, Lau C, Lemon TA, Liang AJ, Liu Y, Luong LT, Michaels J, Morgan JJ, Morgan RJ, Mortrud MT, Mosqueda NF, Ng LL, Ng R, Orta GJ, Overly CC, Pak TH, Parry SE, Pathak SD, Pearson OC, Puchalski RB, Riley ZL, Rockett HR, Rowland SA, Royall JJ, Ruiz MJ, Sarno NR, Schaffnit K, Shapovalova NV, Sivisay T, Slaughterbeck CR, Smith SC, Smith KA, Smith BI, Sodt AJ, Stewart NN, Stumpf K-R, Sunkin SM, Sutram M, Tam A, Teemer CD, Thaller C, Thompson CL, Varnam LR, Visel A, Whitlock RM, Wohnoutka PE, Wolkey CK, Wong VY, Wood M, Yaylaoglu MB, Young RC, Youngstrom BL, Yuan XF, Zhang B, Zwingman TA, Jones AR. Genome-wide atlas of gene expression in the adult mouse brain. *Nature*. 2007; 445:168–176. [PubMed: 17151600]
- Lioy DT, Garg SK, Monaghan CE, Raber J, Foust KD, Kaspar BK, Hirrlinger PG, Kirchhoff F, Bissonnette JM, Ballas N, Mandel G. A role for glia in the progression of Rett's syndrome. *Nature*. 2011; 475:497–500. [PubMed: 21716289]
- Liu Y, Han SSW, Wu Y, Tuohy TMF, Xue H, Cai J, Back SA, Sherman LS, Fischer I, Rao MS. CD44 expression identifies astrocyte-restricted precursor cells. *Dev Biol*. 2004; 276:31–46. [PubMed: 15531362]
- Lovatt D, Sonnewald U, Waagepetersen HS, Schousboe A, He W, Lin JH-C, Han X, Takano T, Wang S, Sim FJ, Goldman SA, Nedergaard M. The transcriptome and metabolic gene signature of protoplasmic astrocytes in the adult murine cortex. *J Neurosci*. 2007; 27:12255–12266. [PubMed: 17989291]
- Lu QR, Sun T, Zhu Z, Ma N, Garcia M, Stiles CD, Rowitch DH. Common developmental requirement for Olig function indicates a motor neuron/ oligodendrocyte connection. *Cell*. 2002; 109:75–86. [PubMed: 11955448]
- Marinescu VD, Kohane IS, Riva A. MAPPER: A search engine for the computational identification of putative transcription factor binding sites in multiple genomes. *BMC Bioinformatics*. 2005; 6:79. [PubMed: 15799782]

- McBurney MW. P19 embryonal carcinoma cells. *Int J Dev Biol.* 1993; 37:135–140. [PubMed: 8507558]
- Meyer-Franke A. Astrocytes induce oligodendrocyte processes to align with and adhere to axons. *Mol Cell Neurosci.* 1999; 14:385–397. [PubMed: 10588392]
- Molofsky AV, Krenick R, Ullian E, Tsai H-H, Deneen B, Richardson WD, Barres BA, Rowitch DH. Astrocytes and disease: A neurodevelopmental perspective. *Genes Dev.* 2012; 26:891–907. [PubMed: 22549954]
- Molofsky AV, Pardal R, Iwashita T, Park I-K, Clarke MF, Morrison SJ. Bmi-1 dependence distinguishes neural stem cell self-renewal from progenitor proliferation. *Nature.* 2003; 425:962–967. [PubMed: 14574365]
- Momose T, Tonegawa A, Takeuchi J, Ogawa H, Umesono K, Yasuda K. Efficient targeting of gene expression in chick embryos by microelectroporation. *Dev Growth Differ.* 1999; 41:335–344. [PubMed: 10400395]
- Muroyama Y, Fujiwara Y, Orkin SH, Rowitch DH. Specification of astrocytes by bHLH protein SCL in a restricted region of the neural tube. *Nature.* 2005; 438:360–363. [PubMed: 16292311]
- Murphy P, Kolstø A. Expression of the bZIP transcription factor TCF11 and its potential dimerization partners during development. *Mech Dev.* 2000; 97:141–148. [PubMed: 11025215]
- Nielsen S, Nagelhus EA, Amiry-Moghaddam M, Bourque C, Agre P, Ottersen OP. Specialized membrane domains for water transport in glial cells: High-resolution immunogold cytochemistry of aquaporin-4 in rat brain. *J Neurosci.* 1997; 17:171–180. [PubMed: 8987746]
- Oldham MC, Horvath S, Geschwind DH. Conservation and evolution of gene coexpression networks in human and chimpanzee brains. *Proc Natl Acad Sci USA.* 2006; 103:17973–17978. [PubMed: 17101986]
- Oldham MC, Konopka G, Iwamoto K, Langfelder P, Kato T, Horvath S, Geschwind DH. Functional organization of the transcriptome in human brain. *Nat Neurosci.* 2008; 11:1271–1282. [PubMed: 18849986]
- Oldham MC, Langfelder P, Horvath S. Network methods for describing sample relationships in genomic datasets: application to Huntington’s disease. *BMC Syst Biol.* 2012; 6:63. [PubMed: 22691535]
- Pantazopoulos H, Woo T-UW, Lim MP, Lange N, Berretta S. Extracellular matrix-glia abnormalities in the amygdala and entorhinal cortex of subjects diagnosed with schizophrenia. *Arch Gen Psychiatry.* 2010; 67:155–166. [PubMed: 20124115]
- Pfrieger FW. Role of glial cells in the formation and maintenance of synapses. *Brain Res Rev.* 2010; 63:1–8. [PubMed: 20434019]
- Pringle NP, Richardson WD. A singularity of PDGF alpha-receptor expression in the dorsoventral axis of the neural tube may define the origin of the oligodendrocyte lineage. *Development.* 1993; 117:525–533. [PubMed: 8330523]
- Pringle NP, Yu W-P, Howell M, Colvin JS, Ornitz DM, Richardson WD. Fgfr3 expression by astrocytes and their precursors: evidence that astrocytes and oligodendrocytes originate in distinct neuroepithelial domains. *Development.* 2003; 130:93–102. [PubMed: 12441294]
- Regan MR, Huang YH, Kim YS, Dykes-Hoberg MI, Jin L, Watkins AM, Bergles DE, Rothstein JD. Variations in promoter activity reveal a differential expression and physiology of glutamate transporters by glia in the developing and mature CNS. *J Neurosci.* 2007; 27:6607–6619. [PubMed: 17581948]
- Roeling TA, Feirabend HK. Glial fiber pattern in the developing chicken cerebellum: Vimentin and glial fibrillary acidic protein (GFAP) immunostaining. *Glia.* 1988; 1:398–402. [PubMed: 2976399]
- Rowitch DH, Kriegstein AR. Developmental genetics of vertebrate glial-cell specification. *Nature.* 2010; 468:214–222. [PubMed: 21068830]
- Sácha P, Zámečník J, Barinka C, Hlouchová K, Vícha A, Mlcochová P, Hilgert I, Eckschlager T, Konvalinka J. Expression of glutamate carboxypeptidase II in human brain. *Neuroscience.* 2007; 144:1361–1372. [PubMed: 17150306]
- Shibata T, Yamada K, Watanabe M, Ikenaka K, Wada K, Tanaka K, Inoue Y. Glutamate transporter GLAST is expressed in the radial glia-astrocyte lineage of developing mouse spinal cord. *J Neurosci.* 1997; 17:9212–9219. [PubMed: 9364068]

- Sofroniew MV, Vinters HV. Astrocytes: Biology and pathology. *Acta Neuropathol.* 2010; 119:7–35. [PubMed: 20012068]
- Song S-Y, Kato C, Adachi E, Moriya-Sato A, Inagawa-Ogashiwa M, Umeda R, Hashimoto N. Expression of an acyl-CoA synthetase, lipidosin, in astrocytes of the murine brain and its up-regulation during remyelination following cuprizone-induced demyelination. *J Neurosci Res.* 2007; 85:3586–3597. [PubMed: 17722065]
- Stolt CC, Lommes P, Sock E, Chaboissier M-C, Schedl A, Wegner M. The Sox9 transcription factor determines glial fate choice in the developing spinal cord. *Genes Dev.* 2003; 17:1677–1689. [PubMed: 12842915]
- Tien A-C, Tsai H-H, Molofsky AV, McMahon M, Foo LC, Kaul A, Dougherty JD, Heintz N, Gutmann DH, Barres BA, Rowitch DH. Regulated temporal-spatial astrocyte precursor cell proliferation involves BRAF signalling in mammalian spinal cord. *Development.* 2012; 139:2477–2487. [PubMed: 22675209]
- Tsai H-H, Li H, Fuentealba LC, Molofsky AV, Taveira-Marques R, Zhuang H, Tenney A, Murnen AT, Fancy SPJ, Merkle F, Kessaris N, Alvarez-Buylla A, Richardson WD, Rowitch DH. Regional astrocyte allocation regulates CNS synaptogenesis and repair. *Science.* 2012; 337:358–362. [PubMed: 22745251]
- Tzeng SF, Bresnahan JC, Beattie MS, de Vellis J. Upregulation of the HLH Id gene family in neural progenitors and glial cells of the rat spinal cord following contusion injury. *J Neurosci Res.* 2001; 66:1161–1172. [PubMed: 11746449]
- Tzeng SF, de Vellis J. Expression and functional role of the Id HLH family in cultured astrocytes. *Brain Res Mol Brain Res.* 1997; 46:136–142. [PubMed: 9191087]
- Tzeng SF, de Vellis J. Id1, Id2, and Id3 gene expression in neural cells during development. *Glia.* 1998; 24:372–381. [PubMed: 9814817]
- Ullian EM, Sapperstein SK, Christopherson KS, Barres BA. Control of synapse number by glia. *Science.* 2001; 291:657–661. [PubMed: 11158678]
- Vallstedt A, Klos JM, Ericson J. Multiple dorsoventral origins of oligodendrocyte generation in the spinal cord and hindbrain. *Neuron.* 2005; 45:55–67. [PubMed: 15629702]
- Walther EU, Dichgans M, Maricich SM, Romito RR, Yang F, Dziennis S, Zackson S, Hawkes R, Herrup K. Genomic sequences of aldolase C (Zeb1) direct lacZ expression exclusively in non-neuronal cells of transgenic mice. *Proc Natl Acad Sci USA.* 1998; 95:2615–2620. [PubMed: 9482935]
- Watkins TA, Emery B, Mulinyawe S, Barres BA. Distinct stages of myelination regulated by γ -secretase and astrocytes in a rapidly myelinating CNS coculture system. *Neuron.* 2008; 60:555–569. [PubMed: 19038214]
- Xu Q, Bernardo A, Walker D, Kanegawa T, Mahley RW, Huang Y. Profile and regulation of apolipoprotein E (ApoE) expression in the CNS in mice with targeting of green fluorescent protein gene to the ApoE locus. *J Neurosci.* 2006; 26:4985–4994. [PubMed: 16687490]
- Yang Y, Vidensky S, Jin L, Jie C, Lorenzini I, Frankl M, Rothstein JD. Molecular comparison of GLT1+ and ALDH1L1+ astrocytes in vivo in astro-glial reporter mice. *Glia.* 2010; 59:200–207. [PubMed: 21046559]
- Zhang B, Horvath S. A general framework for weighted gene co-expression network analysis. *Stat Appl Genet Mol Biol.* 2005; 4:Article 17.
- Zhou Q, Anderson DJ. The bHLH transcription factors OLIG2 and OLIG1 couple neuronal and glial subtype specification. *Cell.* 2002; 109:61–73. [PubMed: 11955447]

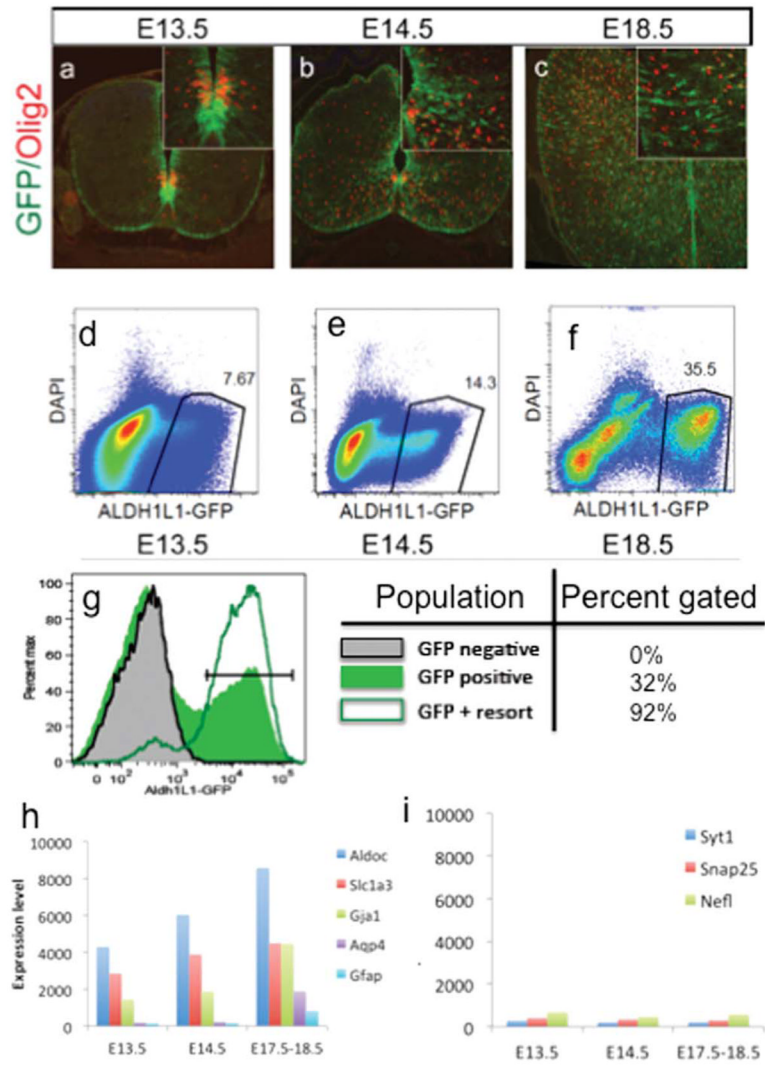


FIGURE 1. Flow-cytometric isolation and microarray profiling of Aldh111-positive cells during spinal cord embryogenesis. **a–c:** Aldh111-GFP and Olig2 expression in spinal cord. **d–f:** Representative flow cytometry plots showing Aldh111-GFP positive populations in E13.5–E18.5 embryos. **g:** Histogram overlay showing an E18.5 GFP-negative control (gray), E18.5 Aldh111-GFP positive sample on first sort (solid green) and the same sample on resort (green line). **h, i:** Expression levels of select astrocytic and neuronal genes.

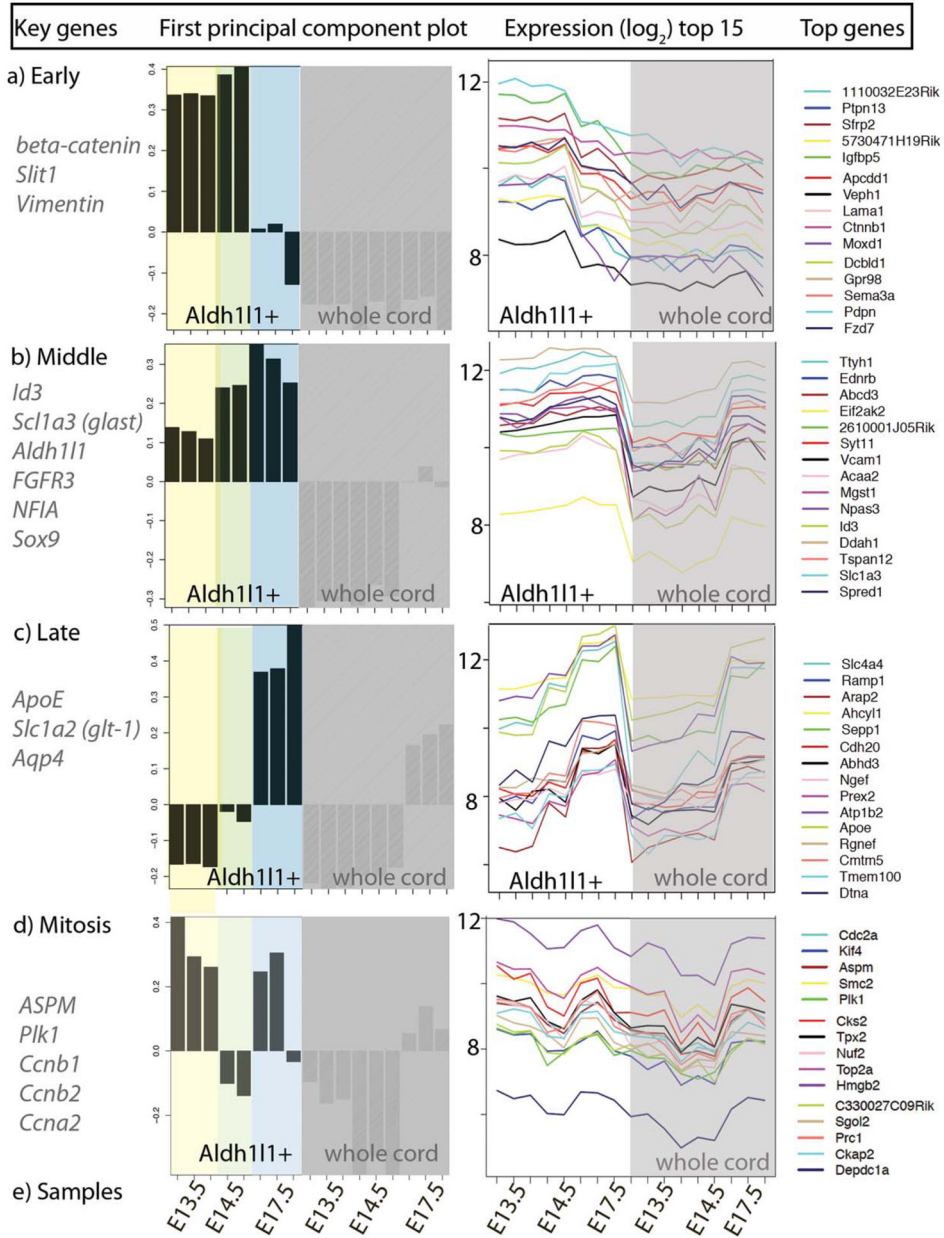


FIGURE 2. Gene coexpression analysis of Aldh111-positive populations reveals temporal waves of glial-specific genes. Left column: bar-plot where each bar represents an individual sample (age listed at bottom (e)) and the y-axis represents the magnitude and direction of the first principal component (a.k.a. the “module eigengene”) for that sample. Samples are grouped into “Aldh111+” and “whole cord”, then arranged chronologically as follows: E13.5 ($n = 3$), E14.5 ($n = 2-3$), E17.5–18.5 ($n = 3$). Right column: lineplot showing expression levels for the top 15 genes on the microarray ranked by their Pearson correlation to the corresponding module eigengene (samples are arranged in the same order). Modules: (a) an “early” embryonic module, (b) a “middle” embryonic module, and (c) a “late” embryonic module; (d) “mitosis” module (e) sample order.

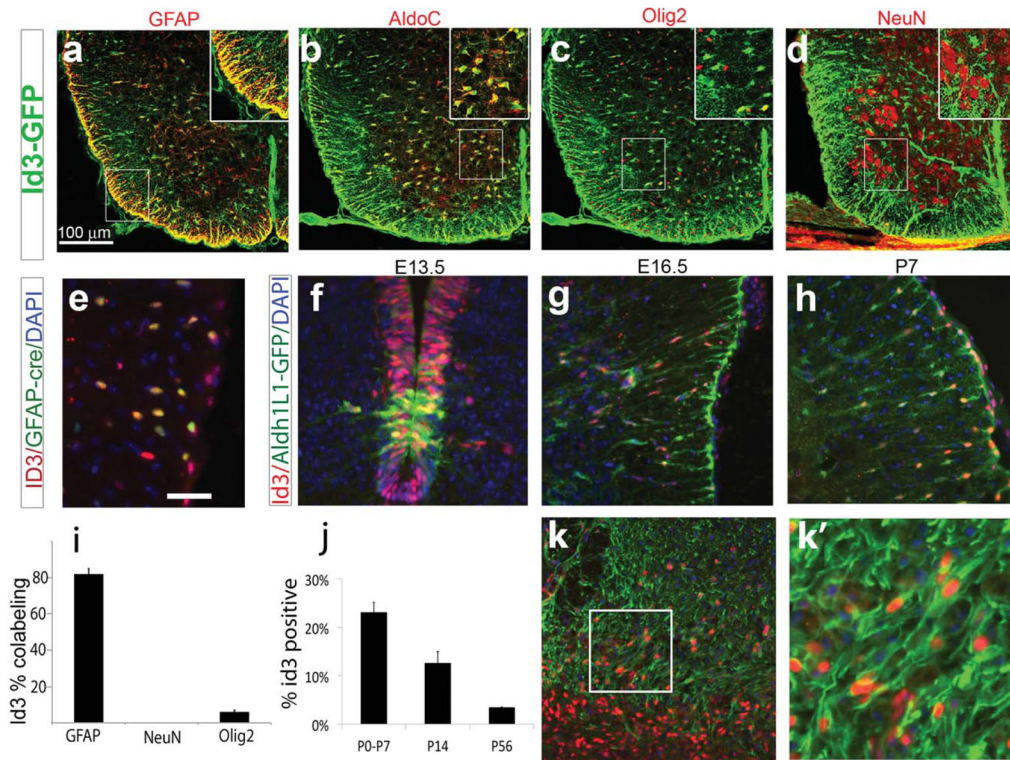


FIGURE 3. Novel reagents for Id3 labeling demonstrate that it is downregulated with astrocyte maturation and re-expressed in reactive gliosis. **a, b, c, d:** Costaining in P1 spinal cord of Id3-GFP (green) and GFAP, AldoC, Olig2, and NeuN antibodies (red). **e:** Costaining of Id3 antibody with GFAP-cre in an hGFAP-cre transgenic mouse. **f, g, h:** Colabeling of Id3 and Aldh1l1-GFP during development (**i**) Coexpression of Id3 with GFAP-cre, NeuN, or Olig2 in spinal cords of transgenic animals expressing hGFAP-cre at P7. (**j**) Downregulation of Id3 with age ($n = 3$ animals, >5 sections per animal). **k, k'** Id3 reactivation in a lysolethicin injury in adult mouse spinal cord 10 days post lesion.

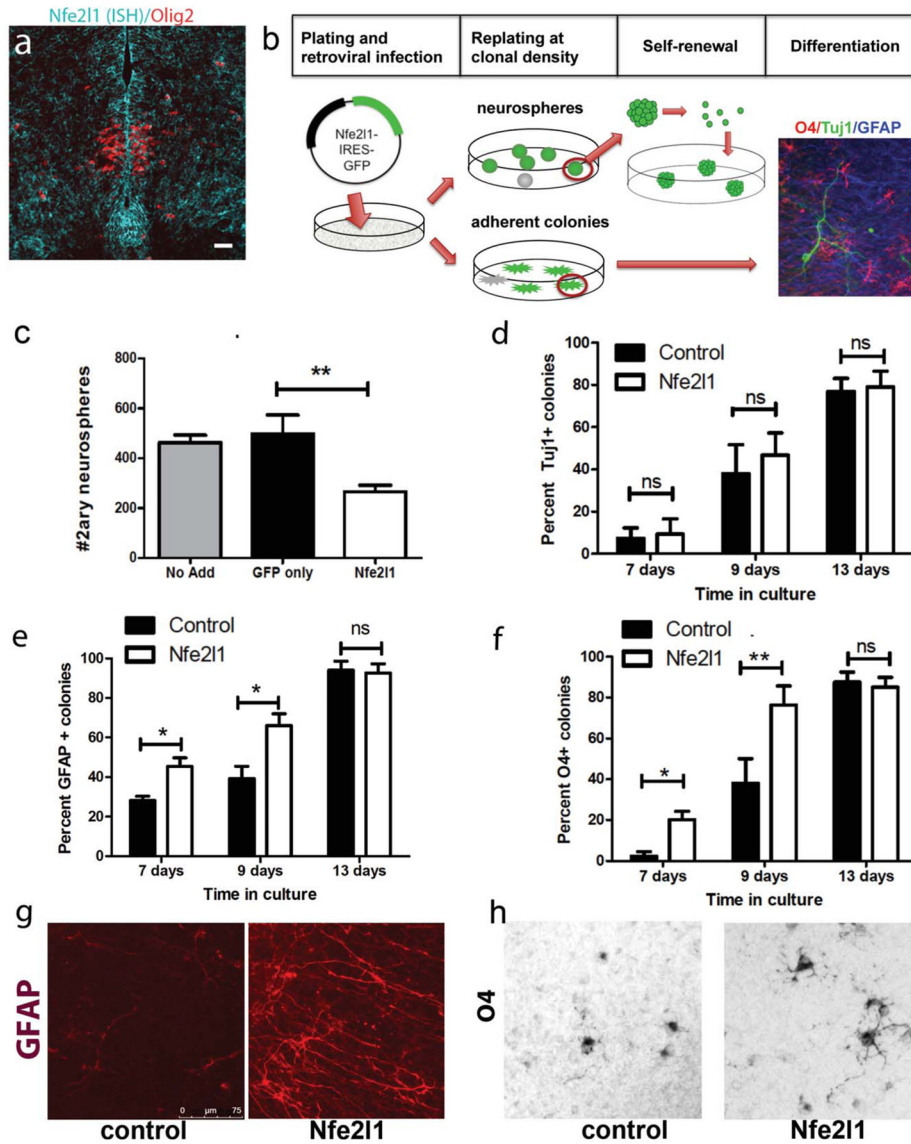


FIGURE 4. Nfe211 is expressed in the ventricular zone in early embryogenesis and promotes glial fate in clonal neural stem cells *in vitro*. **(a)** E13.5 mouse ventral spinal cord with false color *in situ* hybridization for Nfe211 (blue) and Olig2 immunostaining (red). **(b)** Schematic of the clonal neural stem cell assay for testing the instructive role of transcription factors on multipotent progenitors. **(c)** Overexpression of Nfe211 decreases stem cell self-renewal expressed as number of secondary neurospheres generated per primary neurosphere ($P < 0.001$, $n = 3$ independent experiments, 25–30 NS per condition). **(d)** Effect of Nfe211 overexpression on the percentage of colonies expressing the neuronal marker Tuj1. **(e, g)** Nfe211 significantly increases the percentage of colonies that express GFAP at 7 and 9 DIV. **(f, h)** Increase in the percentage and maturity of colonies that express the mature oligodendrocyte marker O4 at 7 and 9 DIV (images in g, h are from 9 DIV). Culture data represents avg \pm SEM from $n = 3$ –4 independent experiments. Control represents cultures infected with GFP-only retrovirus. O4 expression was scored as present/absent. GFAP expression scored as distinctly fibrillar was considered positive. Statistical significance calculated using Student’s t-test for each time point, $*P < 0.05$, $**P < 0.01$.

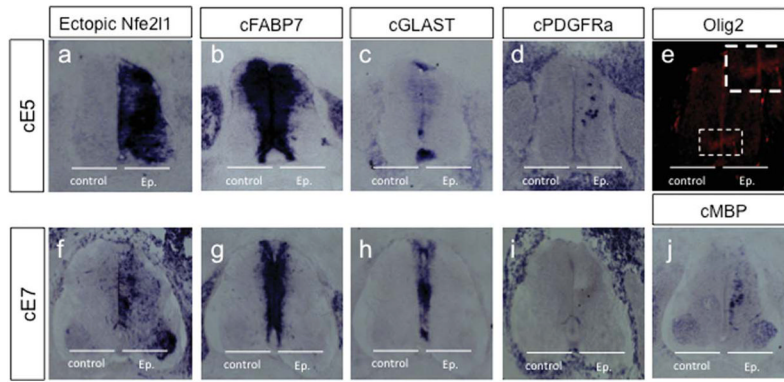


FIGURE 5. Overexpression of Nfe2l1 in early chick neural tube induces expression of some oligodendroglial but not astroglial markers. The right half of chick neural tube was electroporated at embryonic day 2 and harvested at day 5 (a–e) or day 7 (f–j). (a, f) *In situ* hybridization (ISH) for Nfe2l1, (b, g) ISH for FABP7, (c, h) ISH for GLAST, (d, i) ISH for PDGFRA, (e) immunostaining for Olig2 (j) ISH for MBP (in all cases representative images shown are from one of six independent replicates).

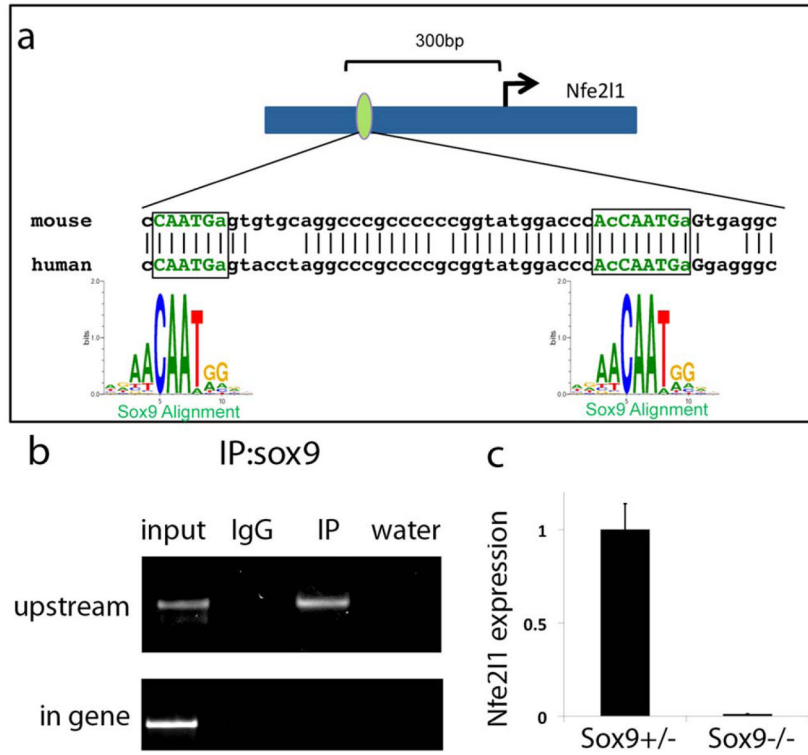


FIGURE 6. Sox9 positively regulates Nfe2l1 expression in multipotent progenitors. **(a)** Diagram of Nfe2l1 promoter region shows two conserved Sox9 sites in mouse and human. **(b)** Immunoprecipitation of a neural stem cell line (P19) with Sox9 antibody demonstrates binding in the Nfe2l1 upstream promoter, but not in the gene sequence. **(c)** Quantitative PCR for Nfe2l1 demonstrates a decrease in Nfe2l1 expression in Sox9-deficient neurospheres relative to heterozygous neurospheres (n = 2 independent experiments). [Color figure can be viewed in the online issue, which is available at wileyonlinelibrary.com.]

TABLE 1

Ingenuity Pathways Analysis of Temporally Distinct Astrocyte Genes

Ingenuity canonical pathway	P-value	Genes
Early module		
Ephrin receptor signaling	0.00138	EPHB1, NRAS (includes EG:18176), ANGPT1, PTPN13, CXCR4
3-phosphoinositide biosynthesis	0.00186	PTPN13, PI4K2B, DUSP16
Axonal guidance signaling	0.00263	SEMA3A, EPHB1, NRAS (includes EG:18176), SLIT1, CXCR4, FZD3, NTN1
ErbB4 signaling	0.00269	NRAS (includes EG:18176), ERBB4, NCSTN
Ephrin B signaling	0.00501	EPHB1, CXCR4, CTNNB1
D-myo-inositol (1,4,5,6)-Tetrakisphosphate biosynthesis	0.00550	PTPN13, DUSP16
D-myo-inositol (3,4,5,6)-tetrakisphosphate biosynthesis	0.00550	PTPN13, DUSP16
Triacylglycerol degradation	0.00603	LIPG, NDST1
Wnt/ β -catenin signaling	0.00813	SFRP2, FZD3, SFRP1, CTNNB1
IGF-1 signaling	0.01096	NRAS (includes EG:18176), IGFBP5, GRB10
Middle module		
Fatty Acid β -oxidation I	0.00001	HADHB, IVD, HSD17B4, ACADM, ACAA2, HADHA
Valine degradation I	0.00001	HADHB, HIBADH, DBT, ALDH6A1, HADHA
Aryl hydrocarbon receptor signaling	0.00014	NR2F1, MGST1, GSTM3, NFIA, TGFB2, ALDH1L1, ALDH6A1, ALDH5A1, ALDH7A1, GSTK1
LPS/IL-1 mediated inhibition of RXR function	0.00032	MGST1, CPT1A, GSTM3, ACOX1, CAT, ALDH1L1, HS3ST1, ALDH6A1, ALDH5A1, ALDH7A1, GSTK1, MAOA
Glutaryl-CoA degradation	0.00068	HADHB, HSD17B4, HADHA
Oleate biosynthesis II (Animals)	0.00120	Scd2, CYB5A, ALDH6A1
Leukocyte extravasation signaling	0.00174	ITGB1, ARHGAP5, GNAI2, TIMP3, VCAM1, EZR, MMP14, JAM2, ACTN4, PRKD1
Methylmalonyl pathway	0.00200	MCEE, MUT
Human embryonic stem cell pluripotency	0.00204	SOX2, FGFR3, NTRK2, BMPR1A, FGFR1 (includes EG:14182), S1PR1, TGFB2, FZD1
Tryptophan degradation X (mammalian, via Tryptamine)	0.00295	ALDH2, ALDH7A1, MAOA
Late module		
GABA receptor signaling	0.00009	SLC6A11, GABBR2, GABRG1, GABRB1, SLC6A1
Fc γ Receptor-mediated phagocytosis in macrophages and monocytes	0.00200	DOCK1, PLD2, TLN2, GPLD1, RAC1
Nicotine degradation II	0.00251	CYP4F8, FMO1 (includes EG:14261), Cyp2j9, CSGALNACT1
Choline biosynthesis III	0.00692	PLD2, GPLD1
Chondroitin Sulfate biosynthesis (Late Stages)	0.00759	CHST2, CHST7, CSGALNACT1
Synaptic long term depression	0.01000	PRKG1, LCAT, ITPR2, GRM3, PPP2R5A
FAK signaling	0.01023	DOCK1, TLN2, RAC1, EGFR
Nicotine degradation III	0.01380	CYP4F8, Cyp2j9, CSGALNACT1
Melatonin degradation I	0.01380	CYP4F8, Cyp2j9, CSGALNACT1

Ingenuity canonical pathway	<i>P</i>-value	Genes
Paxillin signaling	0.01585	DOCK1, TLN2, RAC1, ITGA7

TABLE 2

Top Transcription Factors by Temporal Module

ID	Entrez gene name	P-value
<i>Early module</i>		
Ctmb1	catenin (cadherin-associated protein), beta 1, 88kDa	5.47E-11
Snaip	synuclein, alpha interacting protein	1.40E-09
Nfe2l1	nuclear factor (erythroid-derived 2)-like 1	1.74E-09
BC024139	cDNA sequence BC024139	4.20E-09
Pawr	PRKC, apoptosis, WT1, regulator	1.45E-08
Btaf1	BTA1 RNA polymerase II, B-TFIID transcription factor-associated, 170kDa (Mot1 homolog, <i>S. cerevisiae</i>)	4.20E-08
VeZF1	vascular endothelial zinc finger 1	9.11E-08
<i>Middle module</i>		
Id3	inhibitor of DNA binding 3, dominant negative helix-loop-helix protein	2.36E-12
Taf9b	TAF9B RNA polymerase II, TATA box binding protein (TBP)-associated factor, 31kDa	6.37E-12
Hey1	hairy/enhancer-of-split related with YRPW motif 1	5.65E-11
Etv5	ets variant 5	7.02E-10
Hopx	HOP homeobox	8.27E-10
Rfc1	replication factor C (activator 1) 1, 145kDa	8.89E-10
Nfia	nuclear factor I/A	1.54E-09
Wwtr1	WW domain containing transcription regulator 1	2.95E-09
Klf15	Kruppel-like factor 15	3.36E-09
Trps1	trichorhinophalangeal syndrome I	7.4E-09
Sox9	SRY (sex determining region Y)-box 9	8.16E-09
Sox2	SRY (sex determining region Y)-box 2	3.74E-08
Arnt1	aryl hydrocarbon receptor nuclear translocator-like	6.78E-08
Neo1	neogenin 1	7.96E-08
Maml2	mastermind-like 2 (<i>Drosophila</i>)	8.76E-08
Trip4	thyroid hormone receptor interactor 4	1.85E-07
<i>Late module</i>		
Kank1	KN motif and ankyrin repeat domains 1	3.42E-11
Csda	cold shock domain protein A	1.74E-08
Bcl6	B-cell CLL/lymphoma 6	3.49E-08
Klf9	Kruppel-like factor 9	1.07E-07
Zhx3	zinc fingers and homeoboxes 3	1.25E-07
Hif3a	hypoxia inducible factor 3, alpha subunit	1.40E-07
Kcnip3	Kv channel interacting protein 3, calsenilin	1.44E-07